

EFFECT OF THE LINE-OF-SIGHT INTEGRATION ON THE PROFILES OF CORONAL LINES

N.-E. Raouafi* and S. K. Solanki

Max-Planck-Institut für Aeronomie, 37191 Katlenburg-Lindau, Germany

E-mail: Raouafi@linmpi.mpg.de; Solanki@linmpi.mpg.de

ABSTRACT

We reexamine the interpretation of coronal observations aiming at the determination of the coronal magnetic field and/or the solar wind velocity vectors. In particular we investigate the effect of the integration along the line-of-sight on the profiles of O VI spectral lines emitted in the corona employing a simple model of the large scale coronal magnetic field and solar wind. Here we present preliminary results. We concentrate on the polar coronal holes and find that although the line-of-sight integration is not important at small heights, the width of the emitted line is increasingly affected when moving outwards from the solar disk. At distances of $2.5 R_{\odot}$ and greater the width of the profile integrated along the LOS is more than 2 times as larger as the line profile obtained from an elementary emitting volume on the polar axis.

Key words: Line profiles – Solar corona – Solar wind.

1. INTRODUCTION

The UltraViolet Coronagraph Spectrometer (UVCS) (Kohl et al. 1995) on the Solar and Heliospheric Observatory (SoHO) provided new and surprising results concerning the solar corona, in particular the polar holes. Very broad spectral lines emitted by heavy ions (namely O VI and Mg X) was the most exciting result obtained from UVCS data. In order to interpret these observations together with the total intensity ratio of the O VI doublet, ion cyclotron waves were invoked to propagate through the corona, causing anisotropic velocity distributions (temperature anisotropy) for the heavy ions. The temperature of the heavy ions in the direction perpendicular to the coronal magnetic field are found to be much bigger than those in the direction parallel to the magnetic field ($\frac{T_{\perp}}{T_{\parallel}} > 100$). In addition, the heavy ions

*Associated researcher to the LERMA Department at the Observatoire de Paris-Meudon, France

are deduced to be hotter than the protons. Other important results show that protons are slower than the heavy ions, which means differential acceleration for different coronal species. These results have a big impact on the mechanisms of acceleration and heating of the particles of the solar wind. Thus Li et al. (1998) wrote, “Hence, observations of broad line profiles and a decrease in the line ratio below a value of 1 led Kohl et al. (1997) to conclude that a significant kinetic temperature anisotropy exists for coronal O⁵⁺ at a heliocentric distance of about $2.5 R_{\odot}$.” (For more details see Cranmer et al. 1999a,b,c; Kohl et al. 1999 and other publications related to UVCS).

Li et al. (1998) stated that the observed widths of the line profiles provide a measurement of the ion kinetic temperature in the direction perpendicular to the magnetic field. This statement would be correct if the observed signal were to be dominated by light emitted around the point at which the line-of-sight is closest to the solar surface. The interpretation of Li et al. underestimates the effect of the line-of-sight particularly at high altitudes above the solar limb (more than $2 R_{\odot}$). They argued also that it is necessary to have anisotropy in the ion kinetic temperatures to obtain values near unity or below of the intensity ratio between the O VI lines at $\lambda 1031.92$ and $\lambda 1037.61$.

The interpretation of the observations of the solar corona is not an easy task. The low opacity of the corona implies that the observer collects photons emitted over a large range of distances along the Line-of-sight. This means that the obtained signal is the product of different coronal plasmas with different physical conditions (densities, temperatures, velocities, magnetic field, etc.).

The aim of the present paper is to consider the influence of an improved treatment of the line-of-sight integration on the profiles of spectral lines emitted in the corona in the presence of the fast solar wind. In the present paper, we only present results concerning polar coronal holes and we limit ourself to conditions at minimum activity of the solar solar cycle. In sect. 2 we present briefly the model considered for the calculation of the coronal spectral profiles. In sect. 3 we

present the preliminary results obtained through this model. The results are discussed and our conclusions given in sect. 4.

2. THE MODEL

The main goal of the present work is to determine the importance of a more sophisticated modeling on the interpretation of the off-limb spectral data. Thus, we calculate spectral line profiles emitted in the solar corona taking into account in particular the effect of the integration along the Line-of-sight, but also consider a reasonable representation of the coronal magnetic field and employ an empirically determined electron data (see Doyle et al. 1999a,b).

The frequency-dependant intensity for a given spectral line is obtained through the equation

$$\mathcal{I}(\nu, \theta) = \int_{\text{LOS}} [\mathcal{I}_{\text{elec}}(\nu, \theta) + \mathcal{I}_{\text{rad}}(\nu, \theta)] dZ, \quad (1)$$

where $\mathcal{I}_{\text{elec}}(\nu, \theta)$ is function of the electron density along the line-of-sight and $\mathcal{I}_{\text{rad}}(\nu, \theta)$ is function of incident line profile which is in the solar coronal case the disk emission (transition region, chromosphere, ...) profile. The electronic contribution as well as the radiative one depend on the velocity distribution of the scattering ions through the Doppler redistribution. The radiative part may also depend on the magnetic field but in the present paper we drop down the effect of this latter. In equation (1), dZ means the integration along the line-of-sight.

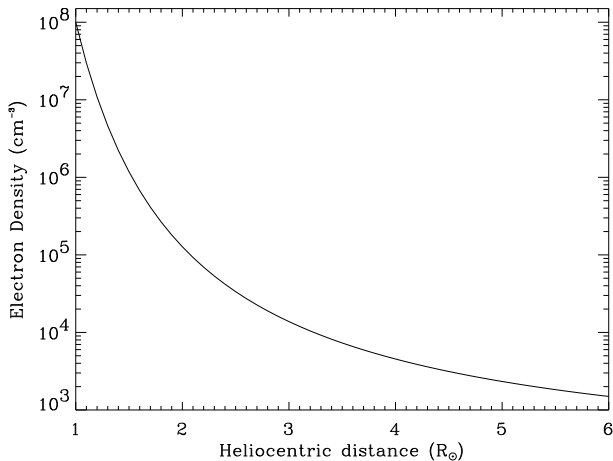


Figure 1. The employed electron density as a function of the distance to the center of the Sun.

To achieve that we consider a simple electron density model for the coronal polar holes similar to that given by Guhathakurta and Fisher (1998) and Doyle et al. (1999a,b). Figure 1 displays the electron density profile as a function of distance to the center of the Sun. Note that this model provides densities that depend only on the distance to the center of the Sun. The influence of other models, providing different variations of the electron density in the corona, will be discussed elsewhere.

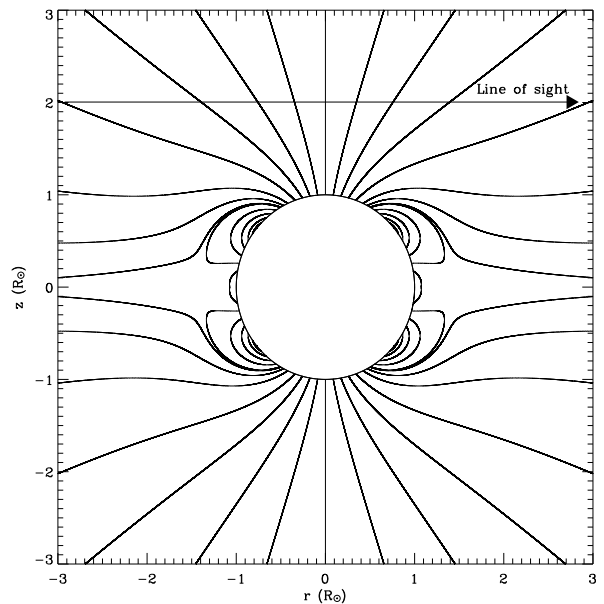


Figure 2. Field lines of the coronal magnetic field for the minimum of solar activity obtained with the model by Banaszekiewicz et al. (1998).

It is known that in the lower corona, the plasma is frozen in the magnetic field lines (plasma $\beta \ll 1$), so that the solar wind flows in directions specified by the field lines. Then in order to determine the solar wind velocity field vector (the macroscopic velocity vector \mathbf{V} of the scattering ions, equation 3) one needs to know the magnetic field vector at all locations along the line-of-sight. For the large scale coronal magnetic field we consider an analytic model by Banaszekiewicz et al. 1998 (see Figure 2). The present model is axisymmetric around the polar axis of the Sun. It is valid for the coronal conditions at the minimum of solar magnetic activity. Smaller scale magnetic structure is neglected here. Note in Figure 2 that the open flux spreads superradially, leading to a large line-of-sight velocity.

The absolute outflow speed of the solar wind is obtained through the mass and magnetic flux conservation equations which are given by

$$\begin{aligned} A(r_0) Ne(r_0) V(r_0) &= A(r) Ne(r) V(r) \\ A(r_0) B(r_0) &= A(r) B(r), \end{aligned} \quad (2)$$

$A(r_0)$, $Ne(r_0)$, $V(r_0)$, $B(r_0)$ are respectively the cross section of the magnetic flux, the electron density, the outflow speed of the ions and the coronal magnetic field at the base of the solar corona (Solar surface). $A(r)$, $Ne(r)$, $V(r)$, $B(r)$ are the same quantities at distance r from the center of the Sun. The direction of \mathbf{V} at a given point on the line-of-sight is that of \mathbf{B} (note the magnetic vector can be oriented toward or away from the solar disk, the solar wind vector is always directed outwards).

For the present work, we assume a simple Maxwellian velocity distribution for the scattering ion that is

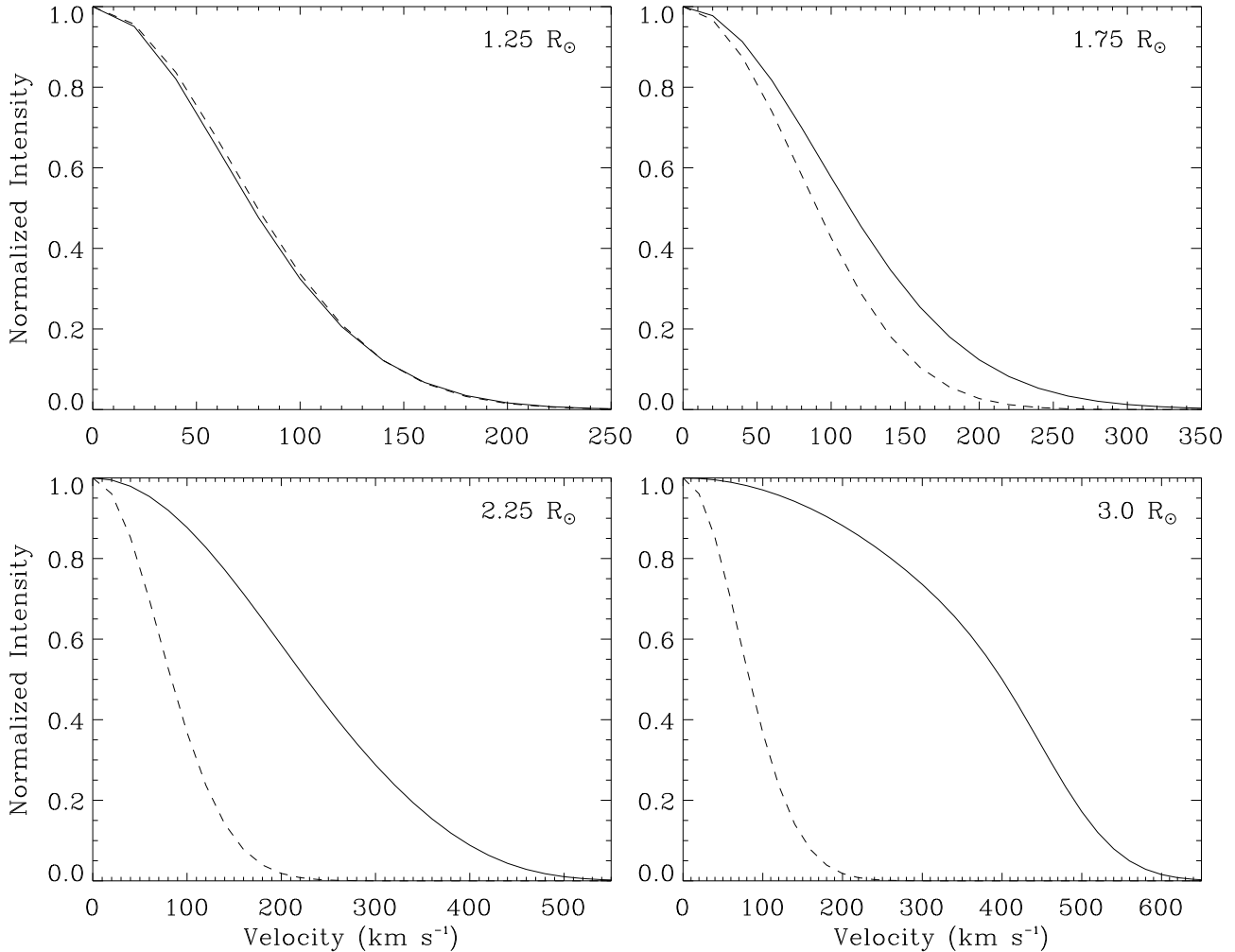


Figure 3. Solid curves are the line-of-sight integrated profiles corresponding to different heights above the solar surface in the different frames. Dashed curves are the correspondent profiles arising from an elementary emitting volume on the polar axis. All profiles are obtained assuming a constant width of 100 km s^{-1} for the Maxwellian velocity distribution of the scattering ions. In order to compare the two profiles (solid and dashed), all profiles have been normalized to their maximum intensities.

given by

$$F(\mathbf{v}) = \frac{1}{\pi^{3/2} \alpha_S^3} \exp \left[- \left(\frac{\mathbf{v} - \mathbf{V}}{\alpha_S} \right)^2 \right], \quad (3)$$

where \mathbf{v} is the atomic velocity field vector. We assume also a Gaussian profile for the radiation coming from the solar disk that is given by

$$\mathcal{I}_i(\nu) = \frac{I_C f(\alpha, \beta)}{\sqrt{\pi} \alpha_i} \exp \left[- \left(\frac{\nu - \nu_0}{\alpha_i} \right)^2 \right], \quad (4)$$

where I_C is the specific intensity emitted at the center of the solar disk; $f(\alpha, \beta)$ is the limb-brightening function; ν_0 is the central frequency of the considered line and α_i is the width of the incident line profile.

3. RESULTS

In order to show clearly the effect of the integration along the line-of-sight on the line profiles, we first

assume that the width of the Maxwellian velocity distribution of the scattering ions does not change with height above the solar limb. This is not physically correct and in a second stage we will allow this width to change with distance to the center of the Sun.

Figure 3 displays line profiles obtained after the integration along the line-of-sight for different heights above the pole (solid lines). The dashed curves are the profiles emitted from a small area around the polar axis (without integration along the line-of-sight).

At very small heights above the limb the local and line-of-sight integrated line profiles are very similar. This can be explained by the fact that the density drops very quickly near the solar surface (see Figure 1). Equally important is that the solar wind speed is small at low heights. Almost the whole observed profiles is formed just above the pole, so that one does not need to integrate along the line-of-sight at these heights. However, when moving away from

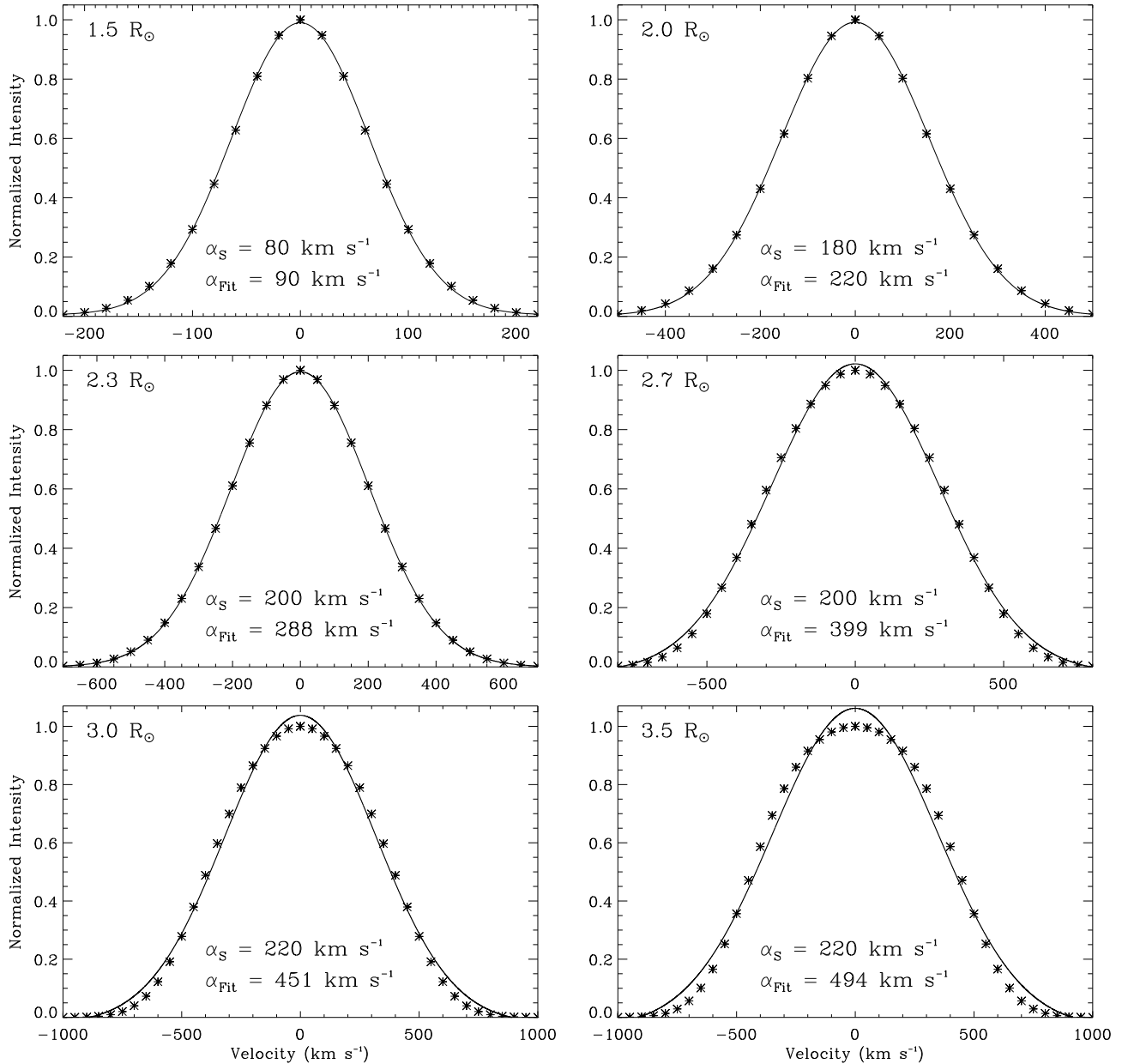


Figure 4. Asterisks are the line-of-sight integrated profiles of the O VI $\lambda 1031.92$ line. These are calculated for different heights above the solar limb. For each height we considered a Maxwellian velocity distribution for the scattering ions with width given by α_S . We assume that this width does not change when moving along the line-of-sight. The obtained profiles are fitted by single Gaussians (solid curves). The widths of these fits are given by α_{Fit} . The corresponding profiles of the O VI $\lambda 1037.61$ line are similar.

the solar disk, the obtained line-of-sight integrated profiles are increasingly wider than the local profiles (dashed curves). The difference between the line-of-sight integrated and non-integrated profiles (in terms of widths) increases dramatically with distance to the solar limb. This is due to the fact that at high altitudes above the limb the solar wind becomes fast enough to get out of the resonance. Thus only the electronic contribution is present and since this latter shifts more than the radiative one we obtain wider profiles.

In order to compare with the observations performed by SoHO/UVCS, we determine for each height (each

line-of-sight) the value of the (turbulence) velocity distribution that gives line profiles with widths comparable with that observed by UVCS. Here also we assume that for each height above the solar limb the width of the velocity distribution does not change when moving along the line-of-sight. This means a “constant turbulence” for each line of sight. More reasonable would be to consider a variable turbulence with the height. This is not taken into account in the present paper, but will be in future work.

We calculate also the total intensity ratio of the O VI doublet lines ($\lambda 1031.92$ and $\lambda 1037.61$). We take into account the effect of the solar wind (Doppler

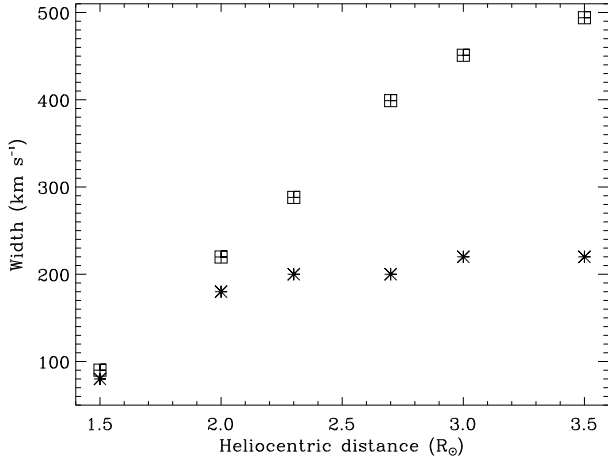


Figure 5. Variation of the line-of-sight integrated line profiles as a function of the heliocentric distance (crossed-squares). Asterisks give the correspondent values of the velocity distribution α_S used to obtain these results. It is clear that the line-of-sight integration is very important at high altitudes. It has almost no effect when very close the Sun surface (below $1.5 R_{\odot}$). Values obtained at heights between $2.0 R_{\odot}$ and $2.5 R_{\odot}$ are a bit smaller than the observed ones. This is due to the electron distribution and to the influence of this latter on the solar wind speed.

dimming) and also the optical pumping of the O VI $\lambda 1037.61$ line by the chromospheric C II doublet ($\lambda 1036.3367$ and $\lambda 1037.0182$). This effect is important above $\sim 2 R_{\odot}$ where the solar wind speed reaches values that enable this process to occur. We assume in particular that the limb-brightening for the C II lines is the same as for the O VI doublet. The latter is measured by SUMER (see Raouafi et al. 2002). We assume that incident line profiles (coming from the solar disk) and the ones emitted at any location in the solar corona are all Gaussians. The widths and intensities of the O VI and C II lines on the disk are those used by Li et al. (1998).

Figure 4 displays line profiles of the O VI $\lambda 1031.92$ calculated at different heights above the solar limb for which observations and results by UVCS are given. A Gaussian fit is applied to each profile (solid curves). The obtained widths and also those used to reproduce those profiles (the widths of the velocity distribution α_S) are given in the same Figure and plotted versus projected distance from the Sun centre of the line-of-sight in Figure 5. At small heights the observed widths are reproduced without difficulty. At large heights ($> 2.5 R_{\odot}$) the obtained widths are comparable to those observed by UVCS. However, between 2 and $2.5 R_{\odot}$ the obtained widths are slightly smaller than the observed ones. This is probably due to the density model which may not fit the real density at those heights.

Figure 6 displays the total intensity ratio of the O VI doublet. UVCS observations are generally very well reproduced. This ratio exhibits a marked dependence on radial distance being well over 2 close to the

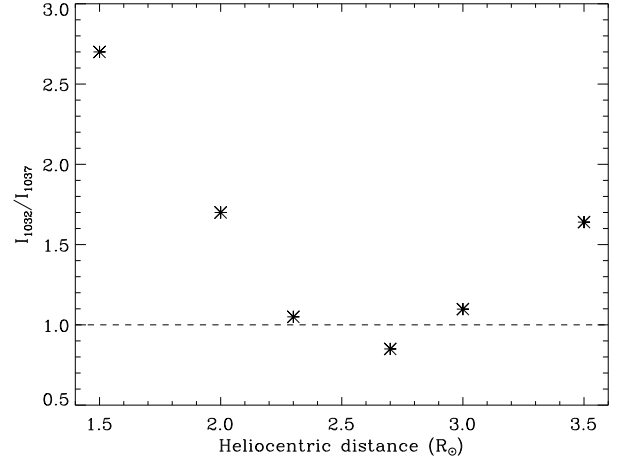


Figure 6. The line-of-sight integrated total intensity ratio of the O VI doublet (I_{1032}/I_{1037}) lines as a function of the distance to the center of the Sun. The behavior of this ratio is similar to that obtained from observations performed by UVCS (see Cranmer et al. 1999). In particular values below 1 can be obtained without any anisotropy in the velocity distribution of the scattering ions (ion temperature anisotropy).

Sun, then dropping rapidly to reach a minimum near $2.5 R_{\odot}$, before increasing again. In particular values below 1.0 are obtained without any anisotropy in the kinetic temperature of the scattering ions. These results can be improved by using better models for the densities, magnetic field and consequently the solar wind. But generally the line-of-sight integration has a very important impact on the obtained profiles and intensity ratio. This effect must be taken into account seriously when interpreting the coronal observations.

4. DISCUSSION

We have considered the effect of line-of-sight integration on spectral lines of O VI emitted in the solar corona in the presence of a consistent model of the large scale magnetic field and solar wind structure. The obtained line widths and total intensity ratios of the O VI doublet at different heights in the coronal polar holes are comparable to those obtained through observations done by SoHO/UVCS, in spite of the fact that we only consider an isotropic kinetic temperature of the scattering ions (namely the O VI). This shows clearly the huge effect of the line-of-sight integration on the profiles and intensity ratios of coronal lines. With more refined models for the coronal densities, magnetic field and solar wind, these results can be improved. These results have also an implication for the importance of anisotropy of kinetic temperature (if there is any) of the heavy ions in the solar corona. This in turn has implications for the mechanisms of heating and acceleration of different species in the polar coronal holes.

REFERENCES

- Banaszkiewicz M., Axford W. I., McKenzie J. F. 1998, *A&A* 337, 940
- Cranmer, S. R., Field, G. B. and Kohl, J. L. 1999a, *ApJ*, 518, 937
- Cranmer, S. R., Field, G. B., Kohl, J. L. 1999b, *Space Science Reviews*, 87, 149
- Cranmer, S. R., Kohl, J. L., Noci, G., et al. 1999c, *ApJ*, 511, 481
- Doyle, J. G., Keenan, F. P., Ryans, R. S. I., Aggarwal, K. M. and Fludra, A. 1999a, *Solar Phys.*, 188, 73
- Doyle, J. G., Teriaca, L. and Banerjee, D. 1999b, *A&A*, 349, 956
- Guhathakurta, Madhulika and Fisher, Richard 1998, *ApJL*, 499, L215
- Kohl, J. L., et al. 1995, *Solar Phys.*, 162, 313
- Kohl, J. L., et al. 1997, *Solar Phys.*, 175, 613
- Kohl, J. L., Esser, R., Cranmer, S. R., et al. 1999, *ApJL*, 510, L59
- Li, X., Habbal, S. R., Kohl, J. L. and Noci, G. 1998, *ApJL*, 501, L133
- Raouafi, N.-E., Sahal-Brchot, S., Lemaire, P., Bomnier, V. 2002, *A&A* 390, 691